

A Two Input Single Output Z-Sourced Dc-Dc Converter for Renewable Applications

Valluri Satya Srinivas¹, E.Vargil Kumar², K.Bhavya³
^{1, 2, 3}, (EEE, Gudlavaleru college of Engg/ Jntuk, India)

Abstract: This paper proposes a double input dc-dc converter based on Z-source converters. In the proposed converter, the input dc voltage can be boosted and also input dc sources can deliver power to the load individually or simultaneously, so combination of a battery with one of the new energy sources such as solar array, wind turbine or fuel cell can be used as input sources. A new control technique individual channel designing is proposed in this to control input supplies of the circuit finally, the simulation results are presented to confirm the theoretical analysis.

Keywords: Z-source converter; double input; dc-dc converter.

I. INTRODUCTION

The renewable energy such as photovoltaic (PV) and wind has created various electric energy sources with different electrical characteristics for the modern power system. In order to combine more than one energy source, such as the solar array, wind turbine, fuel cell (FC) and commercial ac line to get the regulated output voltage, the different topologies of multi input converters (MICs) have been proposed in recent years [1]-[4]. Traditionally, two dc voltage sources are connected to two independent dc-dc power converters to obtain two stable and equivalent output voltages, which are then connected to the dc bus, to provide the electric energy demanded by the load. Another approach for the double-input dc-dc converter is to put two dc sources in series to form a single voltage source where traditional dc-dc power converters can be used to transfer power to the load. In order to transfer power individually, each dc voltage source needs a controllable switch to provide a bypass short circuit for the input current of the other dc voltage source to deliver electric energy continuously [3], [4]. Another approach is to put PWM converters in parallel with or without electrical isolation using the coupled transformer [5]. Control schemes for these MICs with paralleled dc sources are based on the time-sharing concept because of the clamped voltage. Because of the voltage amplitude differences between two dc sources, only one of them can be connected to the input terminal of the dc-dc converter and transfer power to the load at a time [3]. The general form of a MIC consists of several input sources and a single load, conceptually shown in Fig. 1. In general, all of the input sources can deliver power to the load. When only one of the input sources feeds the MIC, it will transfer power to the load individually and the MIC will separate as a PWM Converter.

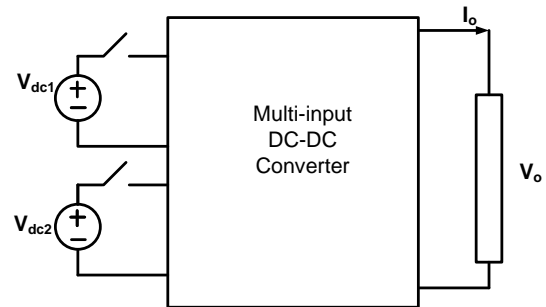


Figure 1. General form of multi input converter

In other words, when more than one input sources are supplied to the MIC, all input sources will deliver power to the load simultaneously without disturbing each other's operation. The objective of this paper is to propose a double-input dc-dc converter which has the following advantages: The dc sources can deliver power to the load individually or simultaneously; the multi winding transformer is not needed; the magnitude of the input dc voltage can be higher or lower than the one with a regulated output; minimum switching devices are used in the converter circuit. The proposed double input dc-dc converter is proper for renewable-energy applications and combination of two different sources (such as battery and photovoltaic or fuel cell).

The purpose of this paper is to introduce the novel Individual Channel Design MATLAB Toolbox and to provide an explanation of how it should be used. At present the software considers only 2x2 control systems. The toolbox is a valuable aid for analysing and designing multivariable control systems. Given a set of specifications for a 2x2 multivariable control system the appropriate use of the toolbox can lead to successful controllers. The process is based on an iterative procedure. Closed loop simulations (in SIMULINK®) are included so results can be tested. Final stability margins and robustness measures are also assessed. The toolbox is inspired on a new approach for multivariable control systems, referred as Individual Channel Design (ICD). ICD is a novel analytical framework that allows the analysis and synthesis of Multi-variable control systems under the context of the Multivariable Structure Function (MSF) by applying classical techniques based on the Bode and Nyquist plots. With the help of this framework it is possible to investigate the potential and limitations for feedback design of any multivariable linear time-invariant control system. Although ICD is in principle a feedback structure based on diagonal controllers, it can be applied to

any cross coupled multivariable system . It is based on the definition of individual transmission channels. In this context the control design is an interactive process that involves the required specifications, plant characteristics, and the multivariable feedback design process itself. Once the channels are defined it is possible to form a feedback loop with the compensator specially designed to meet customer specifications. In this manner the multivariable control design problem is reduced to the design of a single–input single–output control for each channel. ICD has been reported in some control strategies, such asin small scale power networks with embedded generation, in the automotive and the aerospace industry. So far, this toolbox has been used in different control tasks, from induction motors , synchronous generators , to submarines . It has also been employed to provide a design example in a family of plants that range from simple and decoupled to a highly coupled and non– minimum phase one. The document is organised as follows. Section II includes a brief review of ICD. In fact, it is highly recommended to have some expertise in the subject in order to exploit the toolbox successfully. In Section III the design procedure is explained. An introduction to the software and a design example using the toolbox is carried out in Section IV. It is shown in full detail in order to provide a clear demonstration of the toolbox potential. The example here presented corresponds to an interesting and rather challenging design case . Finally, in Section V the conclusions end the paper.

II. CIRCUIT CONFIGURATION AND OPERATION PRINCIPLE OF THE PROPOSED CONVERTER

A.Z-Source Converters

Z-source converters are modern group of power electronic converters which can overcome problems with traditional converters. The Z-source inverter is a novel topology [6] that overcomes the conceptual and theoretical barriers and limitations of the traditional voltage-source converter and current-source converter. The concept of Z-source was used in direct ac-ac power conversion [7]. Similarly, the concept of Zsource also was extended to dc-dc power conversion [8].

B. Circuit Configuration of Proposed Converter

The schematic circuit diagram of the proposed double-input Z-source dc-dc converter with two different voltage sources is shown in Fig. 2. It consists of two different input sources, Vdc1 and Vdc2, and four diodes, S1-S4, applied to provide current path in different states. In this paper, permanent connection of input dc sources is considered, so S1 and S2 can be replaced with active switches if it's required to connect and disconnect each of

sources to input side of converter frequently. Energy receiver, converter and transmitter sections are situated in the middle side of the converter. This section is a two-port network that consists of a split-inductor L1 and L2 and capacitors C1 and C2 connected in x-shape which is named "Z-network". An active switch, S, is situated in output port of Z-network to control input and output power of converter. The final section of converter is a LC filter beside the load in order to reject output signal ripple.

C. Principle Operation of Double Input DC-DC Converter

There are four different operation states with respect to active or inactive states of dc sources. As previously mentioned, both of the input sources can deliver power to the load either individually or simultaneously through the MIC. When only one of the input sources feeds the MIC, it transfers power to the load individually and the MIC will operate as does a PWM converter. Table I summarizes the operation states of the proposed double input dc-dc converter.

D. State 1, both source 1 and source 2 are active

Fig. 3 shows equivalent circuit of this state. When both source1 and source 2 are active, the converter input dc voltage is sum of voltage of two series dc sources, as Fig. 3 and (1) illustrate.

$$V_{in} = V_{dc1} + V_{dc2} \quad (1)$$

In this state, because both two sources are active, S1 and S2 are forward biased and S3 and D4 are reverse biased. Thus, the sources current enters in Z-network through S1 and S2 and after passing load impedance, comes back into sources through negative polarity.

E. State 2, source 1 is active and source 2 is inactive

The equivalent circuit of this state is shown in Fig. 4. In this state, source 1 is active, so only this source provides converter (consequently load) energy. Because of source 1 is active then S1 is forward biased and S3 is reverse biased, so current follows from S1 to Z-network to load.

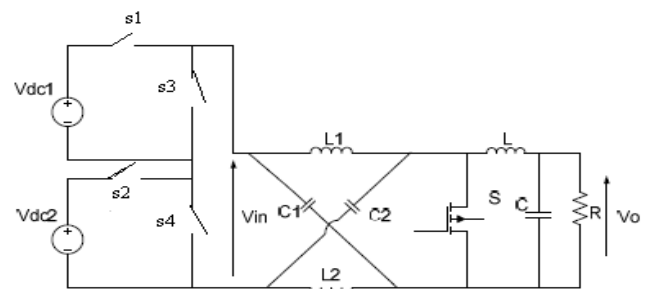


Fig.1 double input z source converter

TABLE I. STATES OF DOUBLE INPUT DC-DC CONVERTER

state	Sources States		Switches States				V_{in}
	V_{dc1}	V_{dc2}	s1	s2	s3	s4	
1	Active	Active	On	On	Off	Off	$V_{dc1} + V_{dc2}$
2	Active	inactive	On	Off	Off	On	V_{dc1}
3	inactive	Active	Off	On	On	Off	V_{dc2}
4	inactive	inactive	Off	Off	On	On	0

In reverse path from load to the source, current can't pass through source 2 and S2, so S4 is forcedly turned on and conduct current to source 1. In this state, converter input dc voltage is only provided by source 1, as (2) shows.

$$V_{in} = V_{dc1} \quad (2)$$

F. State 3, source 1 is inactive and source 2 is active

If source 1 is eliminated for each reason and source 2 is active, the converter can operate normally without effect of source 1 elimination. Fig. 5 shows the equivalent circuit for This state. In state 3, it's only source 2 that supplies converter

And load. Source 2 activation causes forward bias of S2 and Reverse bias of S4. Because of source 1 disconnection, current Passes through S3 and indeed, current turns it on forcedly to Complete current path. In this state, converter input dc voltage is only provided by source 2, as (3) shows.

$$V_{in} = V_{dc2} \quad (3)$$

G. State 4, both source 1 and source 2 are inactive

Basically, this state is only following of one of the previously mentioned three states. Because in this state both dc sources are inactive and disconnected from converter, D1 and D2 are forcedly turned off and consequently, the only existing path for remain current, from previous state, is provided by D3 and D4. Thereupon, in state4 D3 and D4 are turned on. Fig. 6 shows equivalent circuit of this state. Input voltage is zero in this state as shown in (4).

$$V_{in} = 0 \quad (4)$$

Obviously, because both dc sources disconnect from converter, duration of this state is very short and when current descends to zero, whole of converter will be inactive.

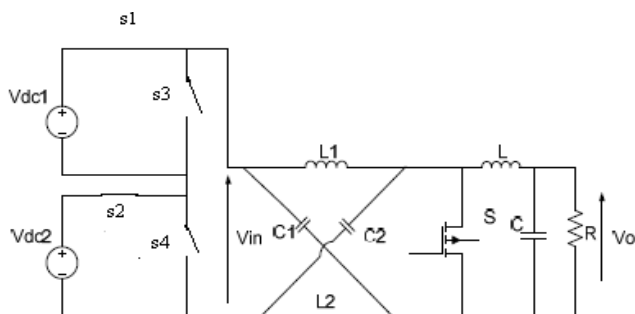


Fig.3 state 1 equivalent circuit

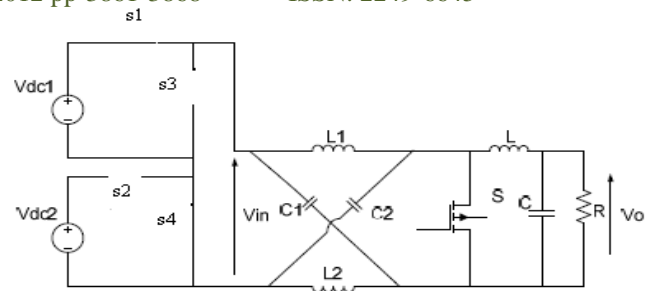


Fig.4 State 2 Equivalent circuit

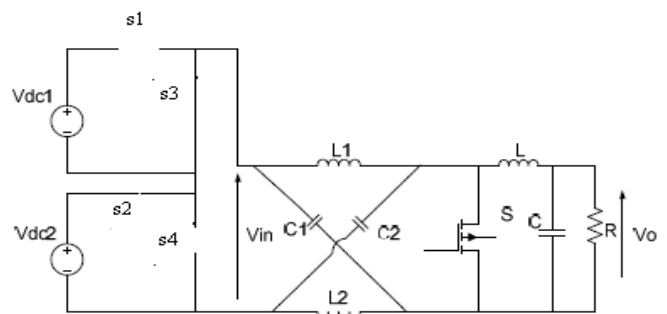


Fig.5 State 3 Equivalent circuit

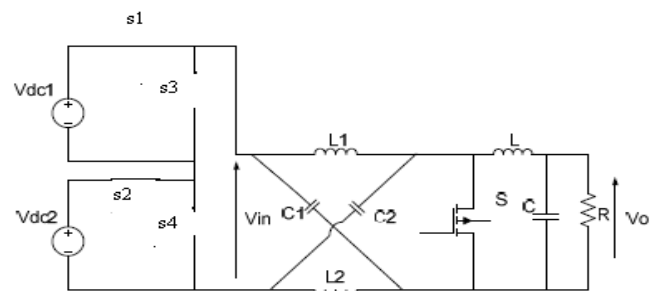


Fig6. State 4 Equivalent circuit

III. STEADY STATE ANALYSIS OF DOUBLE INPUT Z-SOURCE DC-DC CONVERTER

Assuming that the inductors L1 and L2 and capacitors C1 and C2 have the same inductance(L) and capacitance(C), respectively, the Z-source network becomes symmetrical. From the symmetry and the equivalent circuits, we have

$$V_{C1} = V_{C2} = V_C ; V_{L1} = V_{L2} = V_L \quad (1)$$

Given that the inverter bridge is in the shoot-through zero state for an interval of , during a switching cycle T_0 , and from the equivalent circuit, Fig. 6, one has

$$V_L = V_C \quad V_d = 2V_C \quad V_i = 0 \quad (2)$$

Now consider that the inverter bridge is in one of the eight nonshoot-through states for an interval of T_1 , during the switching cycle, . From the equivalent circuit, Fig. 7, one has

$$\begin{aligned} V_L &= V_o - V_C ; v_d = V_o \\ v_i &= V_C - v_L = 2V_C - V_o \end{aligned} \quad (3)$$

Where V_0 is the dc source voltage and $T=T_0+T_1$. The average voltage of the inductors over one switching period(1) should be zero in steady state, from (2) and (3), thus, we have

$$V_L = \bar{v}_i = \frac{T_0 \cdot V_C + T_1 \cdot (V_o - V_C)}{T} = 0 \quad (4)$$

$$\frac{V_C}{V_o} = \frac{T_1}{T_1 - T_0} \quad (5)$$

Similarly, the average dc-link voltage across the inverter bridge can be found as follows:

$$V_i = \bar{v}_i = \frac{T_0 \cdot 0 + T_1 \cdot (2V_C - V_o)}{T} = \frac{T_1}{T_1 - T_0} V_o = V_C \quad (6)$$

The peak dc-link voltage across the inverter bridge is expressed in (3) and can be rewritten as

$$\hat{v}_i = V_C - v_L = 2V_C - V_o = \frac{T}{T_1 - T_0} V_o = B V_o \quad (7)$$

$$B = \frac{T}{T_1 - T_0} = \frac{1}{1 - 2\frac{T_0}{T}} \geq 1 \quad (8)$$

is the boost factor resulting from the shoot-through zero state.

The peak dc-link voltage v_i is the equivalent dc-link voltage of the inverter. On the other side, the output peak phase voltage from the inverter can be expressed as

$$\hat{v}_{ac} = M \cdot \frac{v_i}{2} \quad (9)$$

where is the modulation index. M Using (7), (9) can be further expressed as

$$\hat{v}_{ac} = M \cdot B \cdot \frac{V_o}{2} \quad (10)$$

For the traditional V-source PWM inverter, we have the well known relationship: $v_{ac}=M \cdot V/2$. Equation (10) shows that the output voltage can be stepped up and down by choosing an appropriate buck–boost factor ,

$$B_B = M \cdot B = (0 \sim \infty) \quad (11)$$

From (1), (5) and (8), the capacitor voltage can expressed as

$$V_{C1} = V_{C2} = V_C = \frac{1 - \frac{T_0}{T}}{1 - \frac{2T_0}{T}} V_o \quad (12)$$

The buck–boost factor B_B is determined by the modulation Index M and boost factor B. The boost factor B as expressed in (8) can be controlled by duty cycle (i.e., interval ratio) of the shoot-through zero state over the non shoot-through states of the inverter PWM. Note that the shoot-through zero state does not affect the PWM control of the inverter,

because it equivalently produce the same zero voltage to the load terminal. The available shoot through period is limited by the zero-state period that is determined by the modulation index.

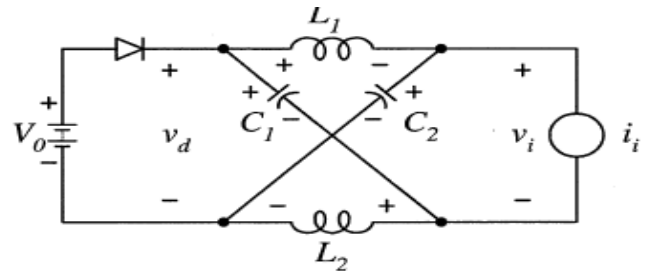


Fig. 7. Equivalent circuit of the Z-source inverter viewed from the dc link.

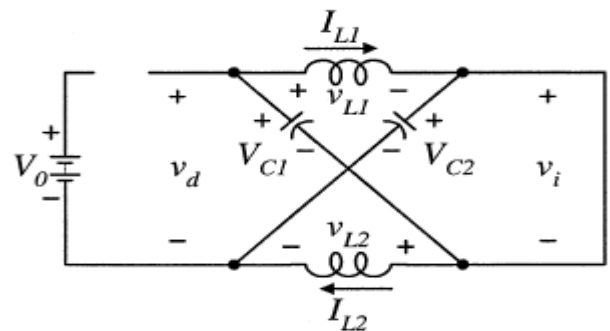


Fig. 8. Equivalent circuit of the Z-source converter viewed from the dc link when the inverter bridge is in the shoot-through zero state.

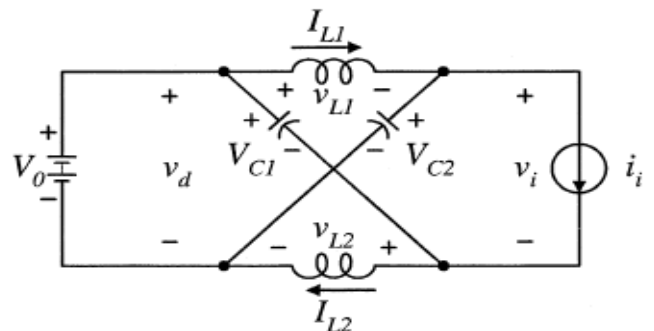


Fig. 9. Equivalent circuit of the Z-source converter viewed from the dc link when the inverter bridge is in one of the eight nonshoot-through switching states.

IV. INDIVIDUAL CHANNEL DESIGNING

In a typical control design task the performance is specified in terms of an output response to a given input. Meanwhile, in multivariable control, there are a number of inputs and outputs and, although it may be clear which inputs are intended to drive which outputs, the design task can be obscured by cross-coupling via the plant dynamics. Nevertheless, for clarity of both performance specification and design, it remains desirable to consider the inputs and outputs in pairs. The situation is depicted in Fig. 1, where \mathbf{G} is the plant and \mathbf{K} is the controller. Input ri is paired with

output y_i in accordance with specifications. An individual pairing is called a *channel*. Then, channel C_i is the pairing between r_i and y_i .

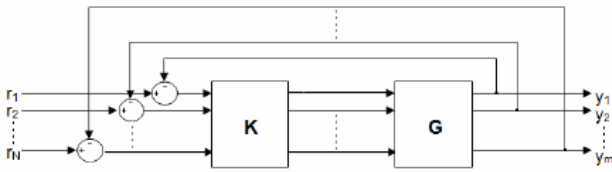


Fig.10 MIMO multivariable system. Channel definition

When the plant cross-coupling is weak, the design task reduces to a set of SISO design tasks and a scalar controller can be designed separately for each channel. In such context, the most appropriate methodology is to apply classical Nyquist/Bode analysis and design to each channel ICD is a framework in which Bode/Nyquist techniques can be applied directly to the channels not only when cross-coupling is weak but in *all circumstances* including when cross-coupling is strong. The multivariable system is decomposed into an equivalent set of SISO systems. Each SISO system is the open-loop channel transmittance between input r_i and output y_i , with the feedback loop between output y_i and input r_i open but all other feedback loops closed, for a particular choice of i . What is particular to Individual Channel Design is that the SISO channel transmittances are reformulated to make explicit the role of the plant structure. Scalar multivariable structure functions (MSFs) to which the individual channel transmittances are simply related encapsulate the significant aspects of the plant structure. The multivariable nature of the original plant is maintained in the equivalent SISO systems through the multivariable structure functions with *no loss of information*. The ICD set up for a 2-input 2-output plant is shown next for completeness. Let a 2x2 plant

$$Y(s) = G(s)U(s) \tag{1}$$

be represented by

$$\begin{bmatrix} y_1(s) \\ y_2(s) \end{bmatrix} = \begin{bmatrix} g_{11}(s) & g_{12}(s) \\ g_{21}(s) & g_{22}(s) \end{bmatrix} \begin{bmatrix} u_1(s) \\ u_2(s) \end{bmatrix} \tag{2}$$

where $g_{ij}(s)$ represents scalar transfer functions, $y_i(s)$ the outputs, and $u_i(s)$ the inputs of the system, with $i, j = 1, 2$. If a diagonal controller is given by

$$u(s) = K(s).e(s) \tag{3}$$

$$\begin{bmatrix} u_1(s) \\ u_2(s) \end{bmatrix} = \begin{bmatrix} K_{11}(s) & K_{12}(s) \\ K_{21}(s) & K_{22}(s) \end{bmatrix} \begin{bmatrix} e_1(s) \\ e_2(s) \end{bmatrix} \tag{4}$$

with $e_i(s) = r_i(s) - y_i(s)$, where $r_i(s)$ represents the plant references, then the open loop input-output channels are clearly defined from Figs. 2 and 3 as

$$C_i(s) = k_{ii}(s)g_{ii}(s)(1 - \gamma_a h_j(s)) \tag{5}$$

where i not equal j and $i, j = 1, 2$. The complex valued function

$$\gamma_a(s) = \frac{g_{12}(s)g_{21}(s)}{g_{11}(s)g_{22}(s)} \tag{6}$$

is referred to as the multivariable structure function (MSF). The functions $h_i(s)$ are:

$$h_i(s) = \frac{k_{ii}(s)g_{ii}(s)}{1 + k_{ii}(s)g_{ii}(s)} \tag{7}$$

The interaction or cross coupling between the channels can be evaluated through a transfer function. For instance, the influence of channel- j on channel- i is

$$d_i(s) = \frac{g_{ij}(s)}{g_{jj}(s)} h_j(s) r_j(s) \tag{8}$$

It is clear that the correct interpretation of the MSF (6) is of great importance because

- It determines the dynamical characteristics of each input-output configuration;
- It has an interpretation in the frequency domain;
- Its magnitude quantifies the coupling between the channels (in the frequency domain);
- It is related to the plant transmission zeros (zeros of $1 - a(s)$, $|G(s)| = g_{11}(s)g_{22}(s) - g_{12}(s)g_{21}(s) = 0$); $a(s) = 1$ determines the non-minimum phase condition;
- Its closeness to $(1, 0)$ in the Nyquist plot indicates to what extent the plant is sensitive to uncertainty in terms of gain and phase margins. This fact plays a key role in order to obtain robust controllers.

A block diagram of the feedback system with the diagonal controller is shown in Fig. 2 and the equivalent scalar channels are shown in Fig. 3.

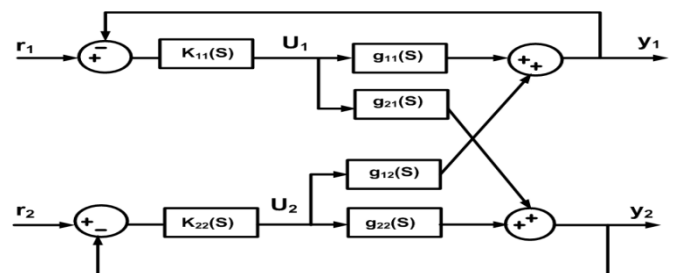


Fig.11 The 2-input 2-output multivariable system with a diagonal Controller

It should be emphasised that in the individual channel representation of the multivariable system there is no loss of information [3]. The multivariable character and cross coupling of the plant are contained in the MSF and the cross coupling terms. That is, (5)–(8) are equivalent to the closed loop matrix function

$$G_d(s) = (I + G(s)K(s))^{-1}G(s)K(s) \tag{9}$$

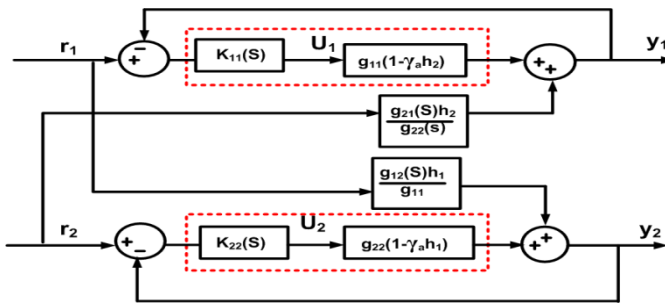


Fig.12 Equivalent channels of a 2-input 2-output control system

It can be proven that in order to stabilise (9) it is just necessary to stabilise the channels given by (5) [7,9]. In general stabilisation of the diagonal elements of $G(s)$ is not required [9]. The open loop system dynamical structure with a diagonal controller is summarised in Table I [3]. Notice that the coupling can be expressed in decibels directly from the channels (5) by means of functions $a(s)hj(s)$. On the other hand, it is possible to determine the dynamical structure of the system using Table I and analysing the Nyquist plot of $(I - a(s)hj(s))$.

Table I. Dynamical structure of open loop channels

Channel	Zeros	Poles
$C_1(s)$	Zeros of $(1-\gamma(s)h_2(s))$	Poles of $g_{11}(s), g_{12}(s), g_{21}(s), h_2(s)$
$C_2(s)$	Zeros of $(1-\gamma(s)h_1(s))$	Poles of $g_{22}(s), g_{12}(s), g_{21}(s), h_1(s)$

It is clear that the controller performance characteristics are determined by the MSF. If the transfer matrix $G(s)$ possess a non-minimum phase transmission zero, some problems will arise while stabilising it especially if the value of the zero is smaller than the desired cut-off frequency. Moreover, the robustness of the channels can be established in terms of gain and phase margins as the Nyquist paths of the functions $ya(s)hi(s)$ do not pass near $(1,0)$. Thus the design of $kii(s)$, which should provide adequate gain and phase margins for $kii(s)gii(s)$, can be obtained through an iterative process. It should be noticed that the RHPPs of the channels are RHPPs of individual transfer functions as established in Table I. On the other hand, the RHPZs of the channels are RHPZs of $(I - y a(s)hi(s))$. Moreover, the number of RHPZs of the previous function can be determined after applying the Nyquist Stability Criterion. In fact, the RHPZs of $(I - \gamma a(s)hi(s))$ are given by

$$Z = N + P \tag{10}$$

where P is the number of RHPPs of $\gamma a(s)hi(s)$ and N is the number of encirclements in clockwise direction to $(1,0)$ of the complex plane in the Nyquist diagram of $y a(s)hi(s)$.

The dynamical structure of the 2x2 plant is determined by the input-output channels defined by pairing each input to each output. For instance:

- (a) $C_1(s) : u_1(s) - y_1(s)$ with $\gamma_a(s) = g_{12}(s)g_{21}(s)g_{11}(s)g_{22}(s)$
 $C_2(s) : u_2(s) - y_2(s)$
- (b) $C_1(s) : u_1(s) - y_2(s)$ with $\gamma_b(s) = g_{11}(s)g_{22}(s)g_{12}(s)g_{21}(s)$
 $C_2(s) : u_2(s) - y_1(s)$

The coupling characteristic of each configuration is determined from $\gamma a(s)$ and $\gamma b(s)$ –their associated MSFs.

V. SIMULATION RESULTS

Simulation of double input Z-source dc-dc converter was performed using MATLAB/SIMULINK to confirm above analysis. Simulation consists of double input circuit with ICD control technique by using z source inverter in this the z source inverter output depends upon the ICD design the because of this reason there is only one operation will be performed which best for the output voltage Converter parameters in the simulation were as in Table II.

TABLE II. Simulation Parameters

Parameter	Value
V_{dc1}	40 V
V_{dc2}	100 V
R	15 Ω
$C1=C2$	1000 μ F
C	500 μ F
$L1=L2=L$	0.5Mh
Switching Frequency	10kHz
Duty ratio (D)	30%

Here the input of double input z source converter are taken as wind and solar energies .for solar input maximum power is achieved by using MPPT algorithm. For wind without MPPT supply is produced to the z source inverter .based upon the out put voltage of load the two inputs are produced for z source converter.

The input of the solar panels as shoen infig.13.In that circuit w are going to apply ICD circit which are taken transfer function as shown beow.the solar out pur currents are shown fig.13.the soalr out put will vry depending upon the required input voltage of the z source converter as well here shown the speed & torque of the wind generator in fig 14.

$$K_{11} = \frac{2}{s^2 + 2s + 1}$$

$$K_{22} = \frac{3}{s^2 + 2s + 1}$$

$$g_{11} = \frac{2}{s^2 + 2s + 1}$$

$$g_{12} = \frac{-2}{s + 1}$$

$$g_{21} = \frac{-1}{s^2 + 2s + 1}$$

$$g_{22} = \frac{6}{s^2 + 2s + 6}$$

approximately zero.the ICD control block is implemented to control the switches at the z at source converter ..

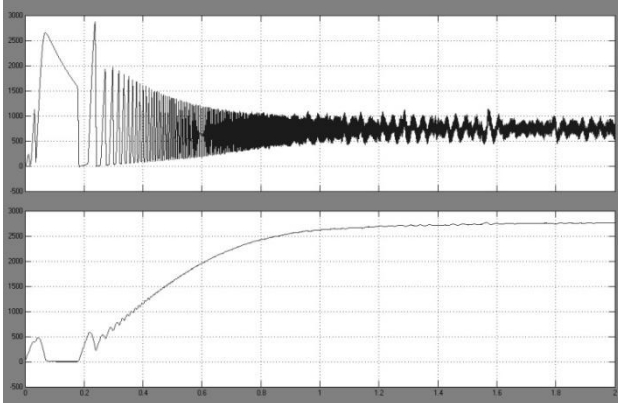
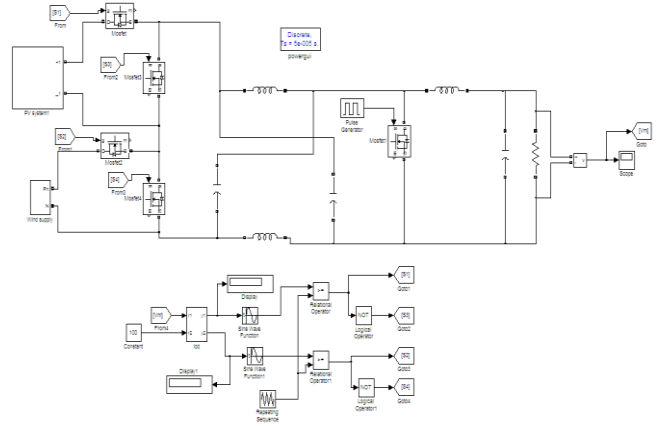


Fig.13a. solar output currents when mppt is not applied & 13b. When mppt is applied

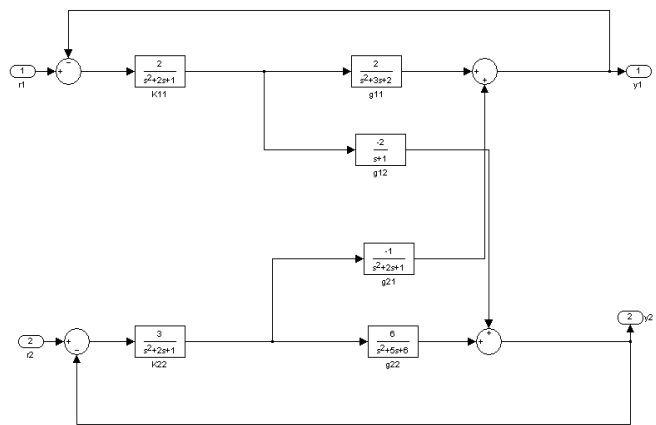


Fig.15 MATLAB simulation of proposed converter along with diagram of the ICD controller

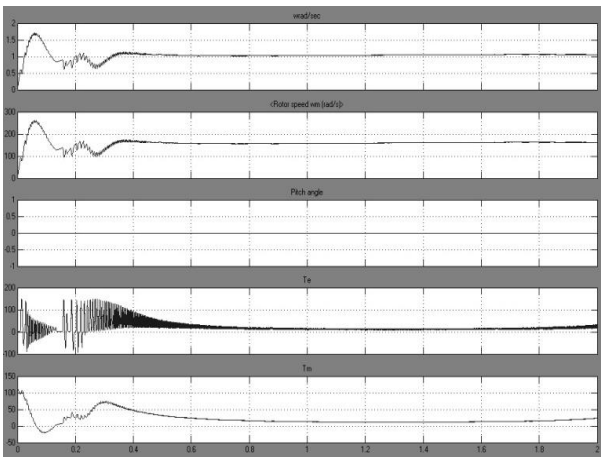


Fig.14 wind speed ,rotor speed, pitch angle, electrical torque .mechanical torque

Here icd control techniqoue is very effiecient technmique.the ICD block diagram i fig.15 .Solar iout pur current is intally is 2700amps but according to requirement we need 800 amps.after applying the MPPT the output of the solar is reduced to nearly 800.wind supply is basecupon the wind speed .rotor speed is given as 150rad/sec and also wind speed is 1rad/sec.the pitch angle is maintained zero always. Electromagnetic torque & mechanical torque maintained

The bode plots of the controller is implemented by the MIMO tool box in MATLAB. The bode plots of the controller.

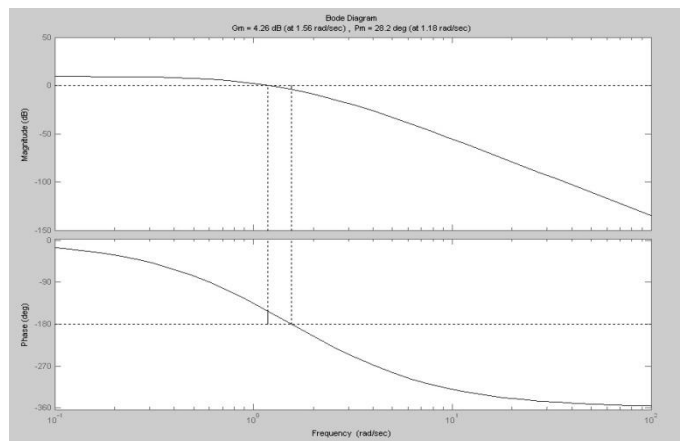


Fig.16(a) bode plot of the K11& K2

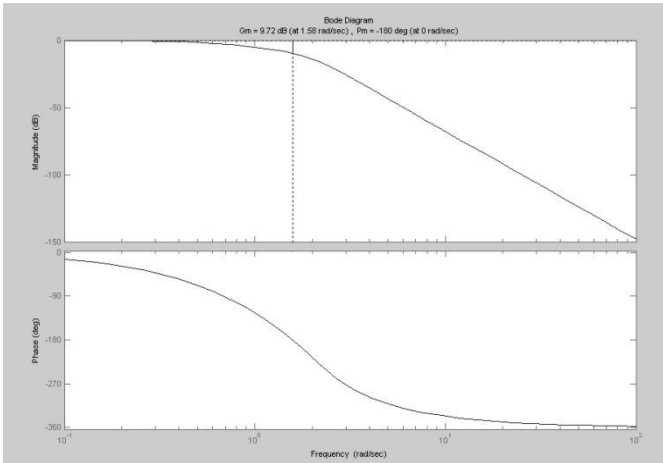


Fig.16(b) bode plot of the K11& K2

Bode gamma plots of the controllers also shown in the fig.17. the performance of the controller is shown in the bode plots to draw the plots we implanted a ICD code which is call as ICD tool is used in MIMO tools.

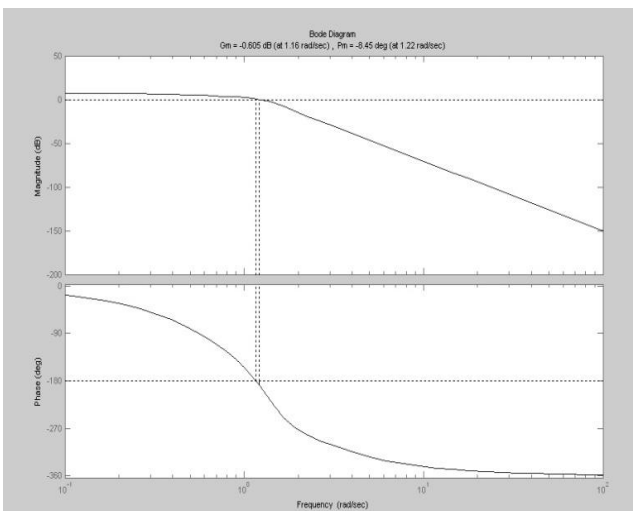


Fig.

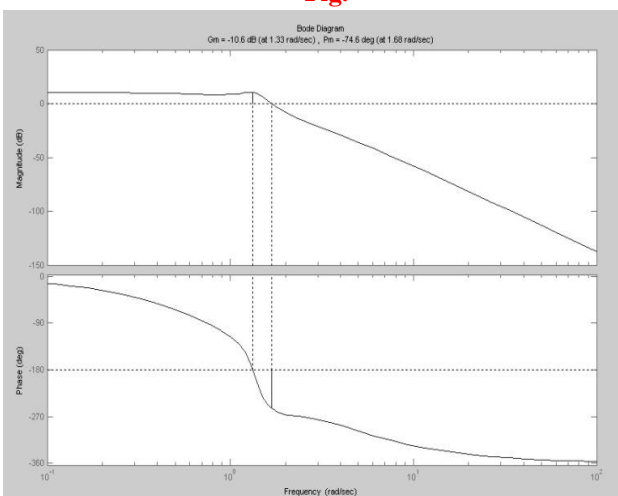


Fig.17 Bode plot gamma of K11 & K22

Finally the output of the is shown in fig.18.the output of te z sources converter is 50V hence the out put will be almost constant after certain time.

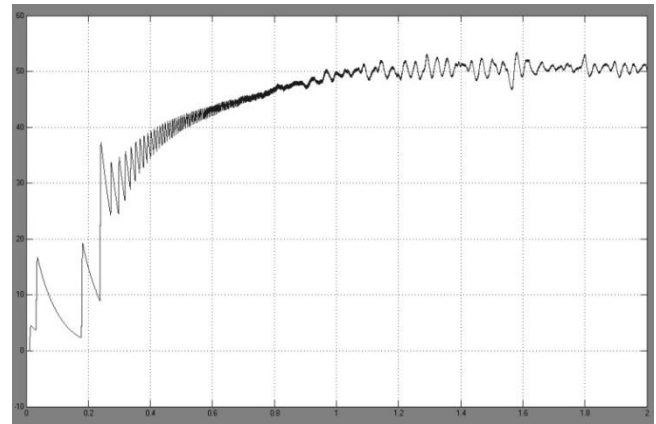


Fig.18 output voltage of the Z-source converter

VI. CONCLUSION

In this paper, double input Z-source dc-dc converter is proposed. The operation principle, ICD controller implementation and its operation and steady-state analysis is explained in detail. The analysis and simulation results show the input dc sources can deliver power to the load, as failure of each input sources doesn't disturb the other's operation.

Two input sources can have different characteristics and voltage. Also, converter controls output power with only one active switch which can reduce cost and improve the reliability. Boosting feature of converter makes it proper for new energy applications.

REFERENCES

- [1] E. Muljadi and H. E. McKenna, "Power quality issues in a hybrid power system," *IEEE Trans. Ind. Appl.*, vol. 38, no. 3, pp. 803-809, May/June 2002.
- [2] F. Giraud and Z. M. Salameh, "Steady-state performance of a gridconnected rooftop hybrid wind-photovoltaic power system with battery storage," *IEEE Trans. Energy Convers.*, vol. 16, no. 1, pp. 1-7, Mar 2001.
- [3] Yaow-Ming Chen, Yuan-Chuan Liu, and Sheng-sien Lin, "Double- Input PWM DC-DC Converter for High-/Low-Voltage Sources," *IEEE Trans. Ind. Electron.*, vol. 53, no. 5, October 2006.
- [4] Yuan-Chuan Liu and Yaow-Ming Chen, "A systematic approach to synthesizing multi-input dc-dc converters" *IEEE Trans. Power Electron.*, vol. 24, no. 1, January 2009.
- [5] H. Matsuo, W. Lin, F. Kurokawa, T. Shigemizu, and N. Watanabe, "Characteristics of the multiple-input dc-dc converter," *IEEE Trans. Ind. Electron.*, vol. 51, no. 3, pp. 625-631, Jun 2004.

- [6] F. Z. Peng, "Z-Source inverter," *IEEE Trans. Ind. Appl.*, vol. 39, no. 2, pp. 504-510, March/April 2003.
- [7] Xu Peng Fang, Zhao Ming Qian, and Fang Zheng Peng, "Single-phase Z-Source PWM AC-AC Converters," *IEEE Power Electron. Lett.*, vol. 3, no. 4, December 2005.
- [8] E. Licéaga-Castro, C.E. Ugalde-Loo, J. Licéaga-Castro, and P. Ponce. "An efficient controller for SV-PWM VSI based on the multivariable structure function". To be presented at: *44th IEEE CDC-ECC*, Spain, 2005.